Structure and Bonding in Cyclic Isomers of $B_2AlH_n^m$ ($n = 3-6$, $m = -2$ to $+1$): A Comparative Study with $B_3H_n^m$, $BAl_2H_n^m$ and $Al_3H_n^m$†

Dibyendu Mallick, Pattiyil Parameswaran,‡ and Eluvathingal D. Jemmis*,#

Department of Inorganic and Physical Chemistry, Indian Institute of Science, Bangalore 560 012, India

Received: May 2, 2008; Revised Manuscript Received: August 17, 2008

The structure, bonding and energetics of $B_2AlH_n^m$ ($n = 3-6$, $m = -2$ to $+1$) are compared with corresponding homocyclic boron, aluminum analogues and $BAl_2H_n^m$ using density functional theory (DFT). Divalent to hexacoordinated boron and aluminum atoms are found in these species. The geometrical and bonding pattern in $B_2AlH_4^-$ is similar to that for B_2SiH_4. Species with lone pairs on the divalent boron and aluminum atoms are found to be minima on the potential energy surface of $B_2AlH_3^{2-}$. A dramatic structural diversity is observed in going from $B_3H_n^m$ to $B_2AlH_n^m$, $BAl_2H_n^m$ and $Al_3H_n^m$ and this is attributable to the preference of lower coordination on aluminum, higher coordination on boron and the higher multicenter bonding capability of boron. The most stable structures of $B_3H_6^+$, B_2AlH_5 and $BAl_2H_4^-$ and the trihydrogen bridged structure of $Al_3H_3^{2-}$ show an isostructural relationship, indicating the isolobal analogy between trivalent boron and divalent aluminum anion.

Introduction

There are few elements in the same group of the periodic table that exhibit such disparities in the hydride chemistry as do the two elements of group 13, boron and aluminum. There are a few known examples of aluminum hydrides such as AlH_3 and Al_2H_6, which are observed in cryogenic matrices[1,2] and in the gas phase.[3] In the solid phase, the alanates such as AlH_4^- and AlH_6^{3-} are observed as their salts.[4] On the other hand, hydrides of boron exhibit a broad diversity of stoichiometries, such as B_2H_6, B_4H_{10}, B_5H_9, B_6H_{10}, $B_{10}H_{14}$, and $B_{20}H_{16}$.[5−8]

This contrasting behavior between boron and aluminum is exemplified even in their three-membered ring compounds. Earlier theoretical studies on the homocyclic three-membered rings of group 13 elements (B, Al, Ga) pointed out the structural diversity of heavier elements as compared to boron hydrides.[9,10] The lone pair on heavy atoms and the out-of-plane distortion of the hydrogen atoms from the plane of the three-membered ring are common in the potential energy surface (PES) of aluminum and gallium species. Several of them are reported experimentally and these highlight the structural differences with their first row analogues. For example, $Na_2[Ga_3R_3]$ and $K_2[Ga_3R_3]$ (R = 2,6-$Mes_2C_6H_3$)[11] have π-delocalization in Ga_3R_3 ring with C_{3h} symmetry.

The recent revival in the chemistry of aluminum[12] especially with the successful synthesis of compounds such as alumino-cyclopropene[12,13] and aluminum analogue of carbene {HC-(CMeNAr)$_2$Al; Ar = 2,6-*i*$Pr_2C_6H_3$}[12,14] point to the exciting possibilities for the future. Our recent report on the structure and bonding in cyclic isomers of $BAl_2H_n^m$ ($n = 3-6$, $m = -2$ to $+1$) emphasized dramatic structural variations in the mixed hydrides containing both boron and aluminum.[15] The nonplanarity of the bridging hydrogens at the B−Al bonds and the stabilization of the π-MO as a function of the number of nonplanar bridging hydrogen atoms are the major highlights of these mixed hydrides. It is interesting to explore the structural variation in $B_3H_n^m$ when boron is systematically substituted by aluminum atoms. The mixed hydrides are exceptionally interesting because they should reflect the relative acidities of the vacant p orbitals on these elements and the relative basicities of the B−H and Al−H bonds. We report here a comprehensive study of all the possible isomers of $B_2AlH_3^{2-}$ and the structures obtained by its sequential protonations, $B_2AlH_4^-$, B_2AlH_5, and $B_2AlH_6^+$. We also present a comparative study among the isomers of the homo and the hetero three-membered cyclic boron and aluminum hydrides to understand the factors that differentiate their hydride chemistry. We expect that an understanding of the smaller clusters would help in the chemistry of larger clusters, and extended solids.

Computational Details

All the structures were optimized using the hybrid HF-DFT method, B3LYP,[16,17] based on Becke's three-parameter functional including Hartree−Fock exchange contribution with a nonlocal correction for the exchange potential proposed by Becke together with the nonlocal correction for the correlation energy suggested by Lee et al. The 6-311++G** basis set was used for all the calculations.[16] The nature of the stationary points was characterized by vibrational frequency calculations. The calculations were done using Gaussian 03 program package.[18] Fragment molecular orbital (FMO)[19a,b] and natural bond orbital (NBO)[19c] methods were used to analyze the bonding in a given structure. In view of the very unconventional nature of the structures **1a**−**f** we have also optimized these structures using the more reliable coupled cluster method, CCSD(T),[20] using the same basis set. Vibrational frequency analysis ensured that the nature of the stationary points remains same at this level of theory as well. The energies were calculated at CCSD(T)/cc-pVTZ for the structures **1a**−**f**. The average error (AE) and the mean absolute deviation (MAD) of the relative energies of $B_2AlH_3^{2-}$ isomers at the B3LYP/6-311++G** as compared to the CCSD(T)/cc-pVTZ level of theory are −1.1 and +2.8 kcal/

† Part of the "Sason S. Shaik Festschrift".

* To whom correspondence should be addressed. Tel: 08022933347. Fax: (+) 91802360-1552. E-mail: jemmis@ipc.iisc.ernet.in.

‡ Present address: Fachbereich Chemie, Philipps-Universität Marburg, Hans-Meerwein-Strasse, D-35032 Marburg, Germany.

Indian Institute of Science Education and Reserch Thiruvananthapuram, CET Campus, Thiruvananthapuram, 695016, Kerala, India.

10.1021/jp803894t CCC: $40.75
Published on Web 10/22/2008

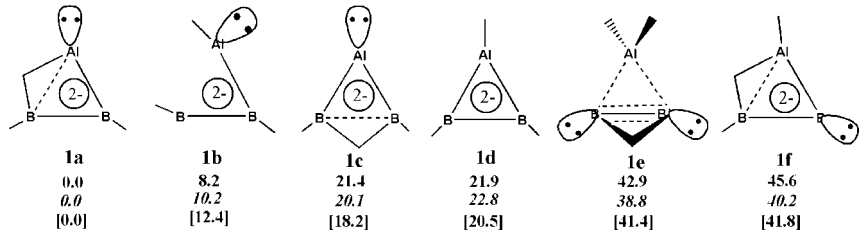

Figure 1. Structures **1a**−**f** and their relative energies in kcal/mol at B3LYP/6-311++G** level of theory (values at CCSD(T)/6-311++G** and CCSD(T)/cc-pVTZ are in italics and within square bracket respectively) for $B_2AlH_3^{2-}$.

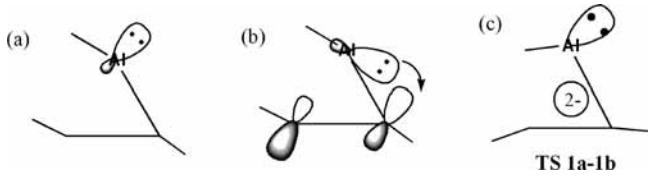

Figure 2. Representations of (a) lone pair on aluminum and (b) a 2c−2e bent Al−B bond. (c) Structure of the transition state for the conversion of **1a** to **1b**.

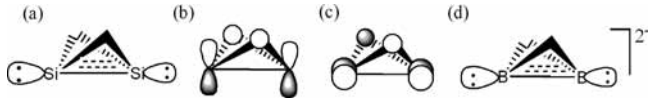

Figure 3. Representations of (a) doubly hydrogen bridged structure of Si_2H_2, (b) and (c) interaction of the bridging hydrogen atoms with the π-MOs of Si_2H_2 and (d) structure of $B_2H_2^{2-}$.

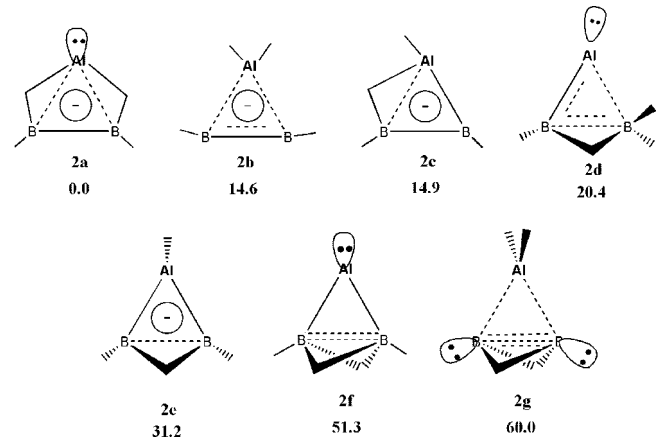

Figure 4. Structures **2a**−**g** and their relative energies (kcal/mol) at B3LYP/6-311++G** level of theory for $B_2AlH_4^-$.

mol, respectively. Similar values for the CCSD(T)/6-311++G** level as compared to the CCSD(T)/cc-pVTZ level of theory are −0.5 and +2.1 kcal/mol, respectively. The results are very much similar and hence structures **2**−**4** were calculated only at B3LYP/6-311++G** level.

Results and Discussion

The structures discussed in this article are obtained by the isoelectronic replacement of the classical D_{3h} geometry of the cyclopropenyl cation by the group 13 elements, viz., one CH group by AlH and the other two CH groups by BH groups. The charges and the number of additional hydrogens are adjusted to give two π-electrons. Various starting geometries for $B_2AlH_3^{2-}$ are obtained by considering all possible combinations of bridging and terminal bonding positions for hydrogen atoms. Similarly, all possible structures are considered for $B_2AlH_4^-$, B_2AlH_5 and $B_2AlH_6^+$, which are the mono-, di- and triprotonated products of $B_2AlH_3^{2-}$. Figures 1 and 4−6 show minimum energy structures of $B_2AlH_3^{2-}$, $B_2AlH_4^-$, B_2AlH_5 and $B_2AlH_6^+$ and their relative energies. All the higher order saddle points and the three-dimensional representations of each structure are given in the Supporting Information.

A variety of bonding situations exist in these compounds ranging from the standard 2c−2e bonds, 3c−2e bonds involving a bridging hydrogen atom and two heavy atoms, 3c−2e bond involving the three heavy atoms in the σ plane and the familiar 3c−2e π-delocalization. There are also several structures with lone pair of electrons and planar tetracoordinate arrangements on heavy atoms. The structural drawings use the following convention to communicate visually the nature of bonding as much as possible.[15] A 2c−2e bond is represented by a solid line. A 3c−2e bond is represented by dotted lines, except those involving the bridging hydrogen. Here, the connectivity between the hydrogen and the main group element is represented by a solid line and the connection between the main group elements is represented by a dotted line. The 2π-electron delocalization is represented by a solid circle inside the three-membered ring. The discussion begins with the structures of $B_2AlH_3^{2-}$ (**1**). The structures obtained by the protonations, $B_2AlH_4^-$ (**2**), B_2AlH_5 (**3**) and $B_2AlH_6^+$ (**4**) are discussed in this order. In view of the large number of minima obtained for **2**, **3**, and **4** these are discussed in relation to the isomers of $B_2AlH_3^{2-}$, **1**. General comparisons are made at the end.

$B_2AlH_3^{2-}$. A variety of unusual bonding arrangements are observed among the many structures which are characterized as minima in energy. We considered 47 different structures in the beginning. Ten of them led to the stationary points on the PES, with six of them characterized as minima and four as first-order saddle points. The schematic representations of all the minimum energy structures of $B_2AlH_3^{2-}$ are shown in the Figure 1. All the higher order saddle points are given in the Supporting Information. The most stable structure **1a** has a planar tetracoordinated boron atom and a lone pair on aluminum atom. Here, a hydrogen atom is bridged between the aluminum and the boron atom. In addition, there are one delocalized π-MO, two 2c−2e B−H, one 2c−2e B−B and one 2c−2e B−Al bonds.

An NBO analysis of **1a** supports this description. The homocyclic boron analogue of **1a** is not a stationary point on the potential energy surface; the classical D_{3h} geometry is the lowest energy structure for $B_3H_3^{2-}$.[9,10] The substitution of one of the BH groups of $B_3H_3^{2-}$ by AlH changes the structure dramatically. The hydrogen attached to Al shifts to bridge a B−Al bond (**1a**). This boron atom is planar tetracoordinated and the aluminum atom has a lone pair. Further substitution of the second BH group by an AlH group results in a structure $BAl_2H_3^{2-}$. The most stable structure of $BAl_2H_3^{2-}$ also has a planar tetracoordinated boron atom and a bridging hydrogen atom between the Al−Al bond.[15] A structure similar to **1a** for $BAl_2H_3^{2-}$ is 9.9 kcal/mol higher in energy than its global minimum energy structure at the B3LYP/6-311+G** level of theory. The most stable structure of $Al_3H_3^{2-}$ is similar to that of $BAl_2H_3^{2-}$. A structure similar to **1a** for $Al_3H_3^{2-}$ is 3.6 kcal/

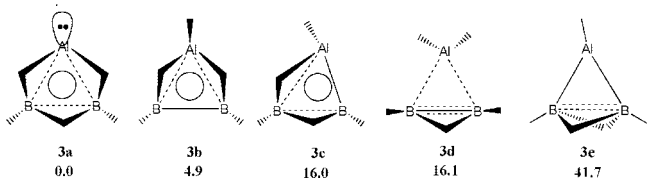

Figure 5. Structures **3a**−**e** and their relative energies (kcal/mol) at B3LYP/6-311++G**, level of theory for B_2AlH_5.

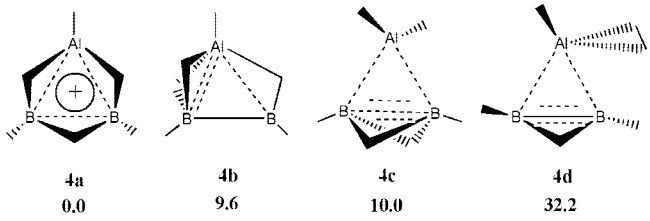

Figure 6. Structures **4a**−**d** and their relative energies (kcal/mol) at B3LYP/6-311++G** level of theory for $B_2AlH_6^+$.

mol higher in energy than its global minimum energy structure.[9] This dramatic structural variation is attributed to the preference of the higher coordination on boron and the lower coordination on aluminum atom.

The next stable structure **1b** is 8.2 kcal/mol higher in energy than **1a**. Here, the AlH and one of the BH groups are reciprocally bent toward each other and the corresponding B−Al bond length (2.43Å) is longer than the other B−Al bond (2.19Å). It is noteworthy that the B−B bond length is shortest (1.49Å) in **1b** among all the isomers of cyclic $B_2AlH_3^{2-}$. The bonding analysis shows that the structure **1b** has a lone pair on aluminum (Figure 2a). Important bonding interactions in this molecule can be visualized by considering the interaction between the HBBH and AlH^{2-} fragments. The B−B bonding in HBBH consists of one σ and one π bond. The sp^n-hybrid lone pair of AlH^{2-} is donated to the vacant in-plane π-MO of the HBBH fragment (Figure 2b) and this interaction is more effective when HBBH is in the trans-bent orientation. This results in a bent 2c−2e bond between aluminum and boron. In addition, it has one 2c−2e Al−H and two 2c−2e B−H bonds. A similar structure is not a stationary point on the PES of $B_3H_3^{2-}$, $BAl_2H_3^{2-}$ and $Al_3H_3^{2-}$. The energy barrier for the conversion of **1a** to **1b** is 11.1 kcal/mol. The structure of the transition state (TS1a-1b) is shown in Figure 2c.

Structure **1c** which is 21.4 kcal/mol higher in energy than **1a**, has a bridging hydrogen atom between two boron atoms, two terminal B−H bonds and a lone pair on the aluminum atom. Here, both boron atoms are planar tetracoordinated. The higher stability of **1a** over **1c** indicates the preference of bridging hydrogen at the Al−B bond than at the B−B bond. The other structural alternative of **1c**, in which boron atom has a lone pair of electrons and hydrogen bridges at the Al−B bond (**1f**), is 24.2 kcal/mol higher in energy than **1c**. The stability order **1a** > **1c** > **1f** is the result of the higher preference of lone pair on aluminum and bridging hydrogen at the B−Al bond. A structure similar to **1c** is a first-order saddle point for the homocyclic boron analogue, but the second most stable structure for the homocyclic aluminum analogue.[9] The highest energy minimum isomer of $BAl_2H_3^{2-}$ has a lone pair on boron and a bridging hydrogen atom at the Al−Al bond.[15]

The classical structure **1d** is 21.9 kcal/mol higher in energy than its most stable structure. A similar structure for $BAl_2H_3^{2-}$ is 21.1 kcal/mol higher in energy than its most stable structure at the B3LYP/6-311+G** level of theory.[15] The molecular orbitals (MOs) of **1d** are similar to the classical Walsh orbitals of the cyclopropenyl cation and it has a delocalized π-MO.

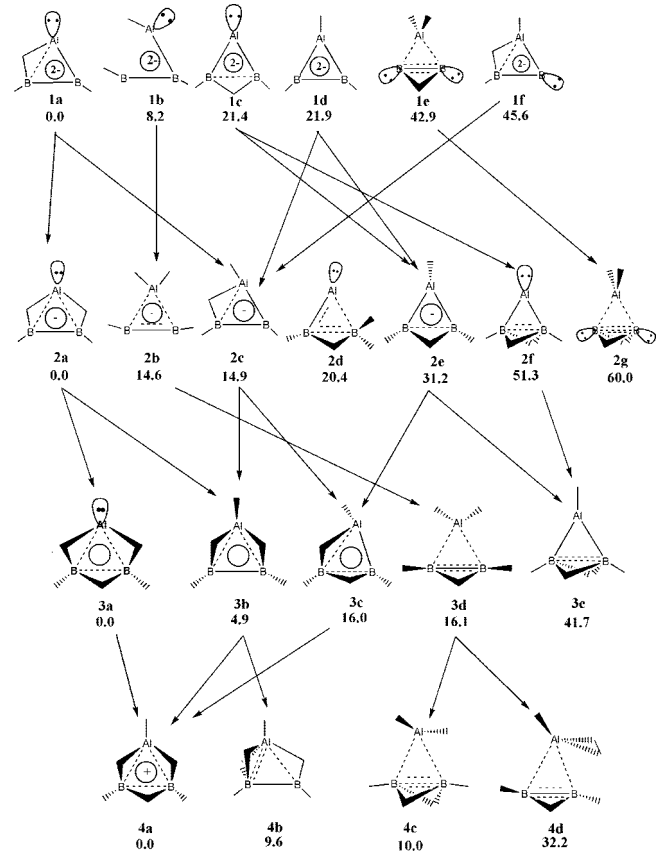

Figure 7. Protonation route of $B_2AlH_n^m$ ($n = 3-6$, $m = -2$ to $+1$) isomers.

The next stable structure **1e** is 42.9 kcal/mol higher in energy than its most stable structure. It has a tetrahedral arrangement around aluminum, out-of-plane bridging hydrogen atom between the boron atoms and a lone pair on each of the boron atoms. The higher relative energy of **1e** can be attributed to the lower preference of lone pair on boron atoms. The bonding in **1e** can be understood by comparing it with the doubly hydrogen bridged structure of Si_2H_2 (Figure 3a).[21] This structure of Si_2H_2 can be formed by protonating the two perpendicular π-MOs in Si_2^{2-} (Figure 3b,c). The isolobal replacement of Si by B^- leads to a similar structure as a minimum on the PES of $B_2H_2^{2-}$ (Figure 3d). The substitution of one of the bridging hydrogen atoms by AlH_2 fragment in $B_2H_2^{2-}$ results in the structure **1e**. The presence of a 2c−2e B−B bond, two 3c−2e B−Al−B and B−H−B bonds and the out-of-plane distortion of the bridging hydrogen atom in **1e** support this bonding description. The angle between BBH and BBAl planes in **1e** is 104.7°. The corresponding angles in Si_2H_2 and $B_2H_2^{2-}$ are 104.1° and 108.9°, respectively.

The analysis of the cyclic isomers of $B_2AlH_3^{2-}$ shows that the structures having lone pair on aluminum atoms have greater preference than those having lone pair on boron atoms.

$B_2AlH_4^-$, B_2AlH_5 and $B_2AlH_6^+$. Figures 4−6 present the minimum energy structures and the relative energies of all the cyclic isomers of $B_2AlH_4^-$, B_2AlH_5 and $B_2AlH_6^+$, respectively. A general relationship among these structures can be obtained by systematic sequential protonation from $B_2AlH_3^{2-}$, as shown in the Figure 7. We have taken the six minimum energy structures of $B_2AlH_3^{2-}$ as the starting point in the protonation route. Arrows indicate a direct structural relationship between the minimum energy structures of $B_2AlH_3^{2-}$, $B_2AlH_4^-$, B_2AlH_5 and $B_2AlH_6^+$ through protonation route.

The number of minimum energy structures decreases as we go from $B_2AlH_3^{2-}$ (six) to $B_2AlH_6^+$ (four). There are several unusual structures that are generated for the mixed B, Al cyclic hydrides. Structures **1a**, **1c**, **1f**, **2a**, **2c** and **4b** have planar tetracoordinate arrangement around boron atoms and **1f**, **2b** and **2c** have planar tetracoordinate arrangement around aluminum atom. The planar tetracoordinate arrangement around boron and aluminum is due to their electron deficiency and hence, they are more flexible to form multicenter bonding as compared to carbon. Structures **2d**, **2f**, **3a**, **3c**, **3e**, **4a,** **4b** and **4c** have pentacoordinate arrangement around boron atoms, whereas **3b** and **4a** have pentacoordinate arrangement around aluminum atoms. Structure **1f** has a lone pair on one of the boron atoms and **1e** and **2g** have lone pairs on both boron atoms. The next perceptible structural aspect is the out-of-plane distortion of bridging hydrogens in these structural series. Structures with one bridging hydrogen atom in the plane of three-membered ring are **1a**, **1c**, **1f** and **2c**, but it is out-of-plane in **1e**, **2d**, **2e**, **3d** and **4d**.

The most stable structure of $B_2AlH_3^{2-}$, **1a**, has three protonation sites: the lone pair on aluminum, the B−B bond and the Al−B bond. The protonation at the Al−B bond gives the structure **2a**, which is the most stable structure of $B_2AlH_4^-$. A similar structure with silicon having a lone pair is most stable for B_2SiH_4.[22] This indicates that the $B_2AlH_4^-$ and the B_2SiH_4 show similarity in structural properties. Schaefer and co-workers also reported similarities between silicon (Si_2H_2) and aluminum hydrides (Al_2H_2).[23] An NBO analysis of **2a** shows that it has two 2c−2e B−H bonds, one 2c−2e B−B bond, two 3c−2e Al−H−B bonds, a lone pair on the aluminum atom and a delocalized π-MO. A similar structure is a first-order and a second-order saddle point for the homocyclic boron and aluminum analogues, respectively.[9] The protonation at the lone pair on aluminum in **1a** gives the structure **2c**, which is 14.9 kcal/mol higher in energy than the most stable structure **2a.** The optimization of the protonated structure at the B−B bond in **1a** leads to the most stable structure **2a**. It indicates that the Al−B bond is more nucleophilic than the B−B bond and the lone pair on aluminum atom.

The structure **2a** can undergo protonation at the B−B bond or at the lone pair on aluminum. The protonation at the B−B bond gives the structure **3a**, which is the most stable structure of B_2AlH_5. It is interesting to note that in **3a**, all the bridging hydrogen atoms are above and the terminal hydrogen atoms are below the plane of the three-membered ring. The planar alternative of **3a** is a second-order saddle point (**3m**) on the PES (see Supporting Information). The higher stability of **3a** over **3m** can be understood by considering their detailed electronic structure. This has been discussed later in greater detail where we have discussed the higher stability of some nonplanar structures over their planar analogues. The distance between the terminal hydrogen (H_t) on boron and the bridging hydrogen (H_b) at the B−B bond is 1.76 Å and that between the terminal hydrogen on boron and the bridging hydrogen at the Al−B bond is 1.94 Å in **3m**. These increase to 2.07 and 2.63 Å, respectively in **3a**.

Addition of H^+ to the lone pair on aluminum in **2a** leads to structure **3b**. Here, the terminal hydrogen atom on aluminum and the two bridging hydrogen atoms are above the plane of the three-membered ring, whereas the terminal hydrogen atoms on boron atoms are below the plane of the three-membered ring. It is 4.9 kcal/mol higher in energy than the most stable structure **3a**. The MO analysis of **2a** shows that the MO corresponding to the lone pair on aluminum (−0.0379 au) is more stable than the delocalized π-MO (−0.0224 au). This supports the higher stability of **3a** over **3b**. The planar alternative of **3b** is a transition state (**3g**, see Supporting Information) for the out-of-plane distortion of the terminal and the bridging hydrogen atoms and the barrier for the interconversion is 3.1 kcal/mol at the B3LYP/6-311++G** level of theory. The nonbonding distance between the terminal hydrogen on boron and the bridging hydrogen at the Al−B bond in **3g** is 1.98 Å; it increases to 2.01 Å in **3b**.

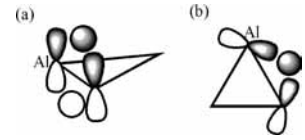

Figure 8. Representations of (a) two out-of-plane bridging hydrogens and (b) an in-plane bridging hydrogen in **4b**.

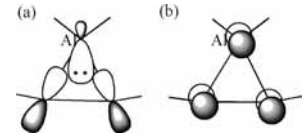

Figure 9. Representations of (a) interaction of the in-plane π-MO of HBBH with the sp^2-hybrid orbital of AlH_2^- fragment (b) delocalized π-MO in **2b**.

The addition of another H^+ ion to **3a** and **3b** results in **4a**, which has three terminal and three bridging hydrogen atoms. This structure is similar to the most stable structure of $B_3H_6^+$.[9] Here, the three bridging hydrogens are above the ring and the two terminal hydrogens on boron atoms are below the plane of the ring. A similar kind of structure is fourth and second most stable structure of $Al_3H_6^+$ and $BAl_2H_6^+$, respectively.[9,15] The planar alternative of **4a** is a second-order saddle point (**4n**, see Supporting Information) on the PES of $B_2AlH_6^+$ and 51.8 kcal/mol higher in energy than the most stable structure. It is interesting to note that in **4n** the distance between the bridging hydrogen atom at the B−B bond and the terminal hydrogen on boron atom is 1.61 Å and that between the bridging hydrogen atom at the Al−B bond and the terminal hydrogen on boron atom is 1.88 Å. These increase to 2.11 and 2.04 Å, respectively in **4a**.

The protonation at the Al−B bond of **3b** results in structure **4b**. It has doubly bridged out-of-plane hydrogen atoms at one Al−B bond and one in-plane bridging hydrogen atom at the other Al−B bond. Here, all the terminal hydrogen atoms are in the plane of the ring. The MO description of **4b** is shown in the Figure 8. Because the Al−H bond is weaker compared to B−H, **4b** is less stable than **4a**.

Similar to **1a**, H^+ can be added to the lone pair on aluminum in **1b**. The addition of proton to the lone pair on aluminum results in the anti van't Hoff structure **2b** in which two hydrogen atoms bonded to aluminum atoms are in the same plane of the three membered ring. Here, the aluminum atom is planar tetracoordinated and the terminal hydrogen atoms on boron are slightly bent toward the aluminum atom. The molecule can be visualized as constructed by the interaction of the HBBH fragment with the AlH_2^- fragment. The in-plane π-MO of HBBH is vacant and it can accept electrons from the sp^2 hybrid orbital of AlH_2^- fragment (Figure 9a). The sp^2 hybrid orbital of Al is less diffused to interact with the π-MO of HBBH, resulting in the bending of the terminal hydrogen atoms on boron toward the AlH_2^- fragment.[24] Similar anti van't Hoff structure for B_2SiH_4 is minimum in the potential energy surface at the B3LYP/6-311++G** level of theory.

The proton can be added to the Al−B bond, lone pair on aluminum or to the B−B bond in **1c**. The protonated structure

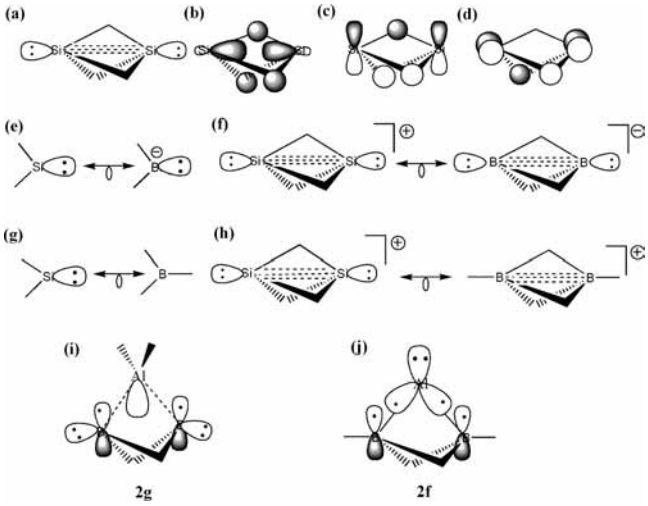

Figure 10. Representations of (a)−(d) bonding description of $Si_2H_3^+$, (e) isolobal analogy between divalent Si and divalent B anion, (f) structural similarities between $Si_2H_3^+$ and $B_2H_3^-$, (g) isolobal analogy between divalent Si and trivalent B atom, and (h) structural similarities between $Si_2H_3^+$ and $B_2H_5^+$ and bonding in (i) **2g** and (j) **2f**.

at the Al−B bond of **1c** leads to **2d** on optimization. It has penta- and tetracoordinated boron atoms. It is interesting to note that the protonation at the lone pair on aluminum atom in **1c** causes out-of-plane distortion of all bridging and terminal hydrogen atoms (**2e**). Its planar alternative **2h** (see Supporting Information) is a transition state for the out-of-plane distortion of the bridging and the terminal hydrogen atoms. The energy barrier for this interconversion is 8.8 kcal/mol. The instability of **2h** can be due to the nonbonded repulsive interaction between the bridging and the terminal hydrogen atoms. The distance between these two hydrogen atoms in **2h** is 1.83Å at the B3LYP/6-311++G** level of theory. The similar distance in **1c** is 1.88 Å. It increases to 1.98 Å in **2e**. Structures similar to **2e** and **2h** are minimum and a first-order saddle point for B_2SiH_4, respectively, at the B3LYP/6-311++G** level of theory.

The protonation at the B−B bond in **1c** leads to a doubly hydrogen bridged structure **2f**. The electronic structure of **2f** consists of two 2c−2e B−H bonds, two 3c−2e B−H−B bonds, two 2c−2e Al−B bonds and a lone pair on the aluminum atom. The structures of **2f** and **2g** can be understood by comparing them with the structure of $Si_2H_3^+$ (Figure 10a). Spectroscopically, $Si_2H_3^+$ is characterized as a triply hydrogen bridged structure.[25] The MO description of $Si_2H_3^+$ is shown in the Figure 10a−d. It can be considered as formed by the interaction of Si_2^{2-} with H_3^{3+}. The σ-MO of Si_2^{2-} can interact with the totally symmetric MO of H_3^{3+} (Figure 10b) and the π-MOs with the other two MOs of the H_3^{3+} (Figure 10c,d).

The isolobal analogy between divalent silicon and trivalent boron atom (Figure 10g) as well as divalent silicon and divalent boron anion (Figure 10e) explains the similarity between $Si_2H_3^+$, $B_2H_3^-$ and $B_2H_5^+$ (Figure 10f,h). Substitution of one of the H^+ in $B_2H_3^-$ by an AlH_2^+ fragment results in the structure **2g** (Figure 10i). Similarly, the substitution of H^+ in $B_2H_5^+$ by Al^- leads to structure **2f** (Figure 10j), which has two 2c−2e Al−B bonds. The lower stability of **2g** over **2f** justifies the lower preference of lone pair on the boron atom as compared to the aluminum atom. A structure similar to **2f** is a minimum for isoelectronic B_2SiH_4 and a second- and a first-order saddle point for homocyclic boron and aluminum analogues.[22,9]

The addition of proton at the Al−B or at the B−B bond of **1d** results in **2c** or **2e**. The higher stability of **2c** over **2e** is due

Figure 11. Representation of structural similarities of (a) Si_2H_2 and (b) B_2H_4.

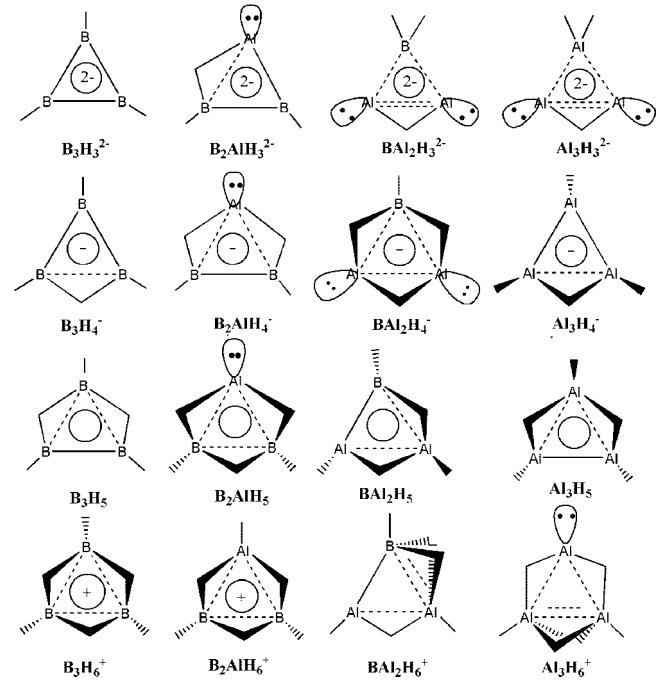

Figure 12. Most stable structures of $B_3H_n^m$, $B_2AlH_n^m$, $BAl_2H_n^m$ and $Al_3H_n^m$ ($n = 3-6$, $m = -2$ to $+1$).

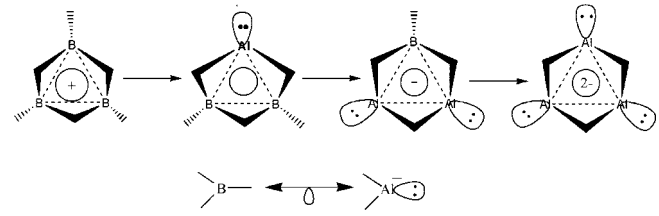

Figure 13. Most stable structures of $B_3H_6^+$, B_2AlH_5 and $BAl_2H_4^-$ and trihydrogen bridged structure of $Al_3H_3^{2-}$ showing isolobal analogy between trivalent boron and divalent aluminum anion.

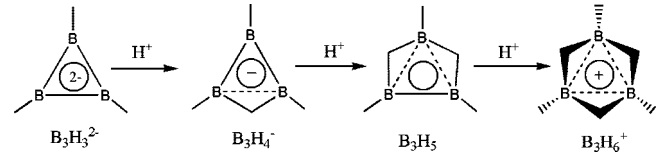

Figure 14. Sequential protonation of $B_3H_3^{2-}$ to $B_3H_6^+$.

the greater nucleophilic character of the Al−B bond as compared to the B−B bond.

The protonation on **2c** at the Al−B bond gives the structure **3b**, whereas the protonation at the B−B bond gives **3c**. In both the structures the terminal and the bridging hydrogen atoms are not in the plane of the three-membered ring. The greater stability of **3b** over **3c** is due to the preference of the bridging hydrogen at the Al−B bond than at the B−B bond.

Structures **3c** and **3e** can be formed by the protonation of **2e** at the Al−B and B−B bonds, respectively. Structure **3e** can also be formed by the protonation at the lone pair on aluminum atom in **2f**. The protonation at the B−B bond in **2b** results in the structure **3d**. The bonding in **3d** can easily be understood by comparing it with the doubly hydrogen bridged structure of Si_2H_2. The isolobal analogy between divalent silicon and

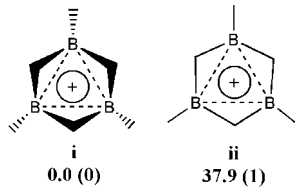

Figure 15. Structures **i** and **ii**, relative energies (kcal/mol) at the B3LYP/6-311++G** level of theory and the number of imaginary frequencies (in parentheses) for $B_3H_6^+$.

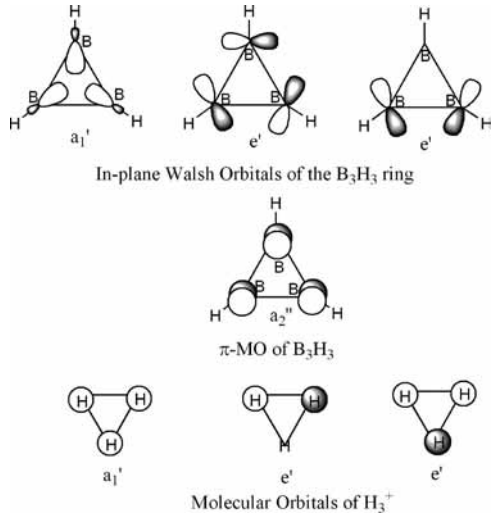

Figure 16. MOs of B_3H_3 and H_3^+ fragments.

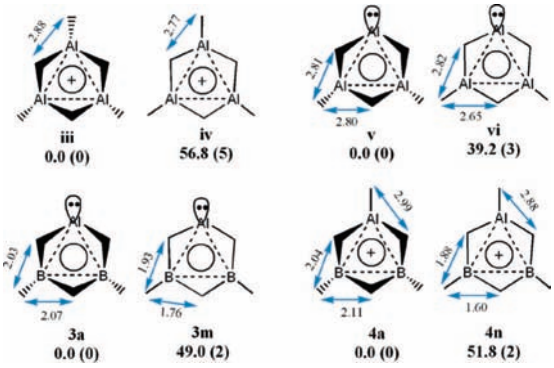

Figure 17. Structures **iii-vi**, **3a**, **3m**, **4a** and **4n**, relative energies (kcal/mol) at the B3LYP/6-311++G** level of theory and the number of imaginary frequencies (in parentheses). The double headed arrows indicate the nonbonded distances (Å) between the terminal and the bridging hydrogen atoms.

trivalent boron explains the similarity in geometry of Si_2H_2 and B_2H_4 (Figure 11).[26] Substitution of one of the bridging hydrogen of B_2H_4 by AlH_2 group results in the structure **3d**.

Even though 14 stationary points are obtained in the PES of $B_2AlH_6^+$, only four of them are found to be minima. Structure **4c** can be visualized as formed by the protonation at the B−B bond in **3d**. Structure **4d** has an unusual structure in which H_2 is attached to the aluminum atom. The H−H distance in **4d** is 0.76Å which is slightly elongated than the H−H distance in H_2.

The most stable structures of $B_3H_n^m$, $B_2AlH_n^m$, $BAl_2H_n^m$ and $Al_3H_n^m$ ($n = 3-6$, $m = -2$ to $+1$) are shown in Figure 12. A dramatic structural alteration is noted when the boron atoms in $B_3H_n^m$ are systematically substituted by aluminum atoms. The most stable structure for $B_3H_3^{2-}$ has a classical D_{3h} geometry.[9,10] Similar structures for $B_2AlH_3^{2-}$, $BAl_2H_3^{2-}$ and $Al_3H_3^{2-}$ are

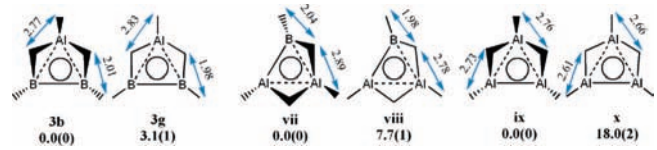

Figure 18. Structures **3b**, **3g** and **vii**−**x**, relative energies (kcal/mol) at the B3LYP/6-311++G** level of theory and the number of imaginary frequencies (in parentheses). The double headed arrows indicate the nonbonded distances (Å) between the terminal and the bridging hydrogen atoms.

higher energy minima on the potential energy surface. Substitution of one of the boron atoms of $B_3H_3^{2-}$ by an aluminum atom alters the most stable structure significantly. It has a bridging hydrogen atom at the Al−B bond and a lone pair on the aluminum atom. This structural alteration is mainly to accommodate the lone pair on the aluminum atom and as a result boron becomes planar tetracoordinate. Further substitution of the second boron atom by an aluminum atom results in $BAl_2H_3^{2-}$. The most stable structure rearranges itself to attain a lone pair on both the aluminum atoms. The most efficient way to do so is by keeping the bridging hydrogen at the weaker Al−Al bond and it results in planar tetracoordinated boron atom. A similar structure is most stable for the homocyclic aluminum analogue but a first-order saddle point for $B_2AlH_3^{2-}$.

The most stable structures of the mono- and diprotonated species of $B_3H_3^{2-}$ have in-plane bridging hydrogen atoms at the B−B bonds. Addition of the third hydrogen results in an out-of-plane distortion of the bridging and the terminal hydrogen atoms. It is interesting to note that the first and the second protonation on the most stable structure of $B_2AlH_3^{2-}$ retain the lone pair on aluminum atom. The di- and triprotonated structures, B_2AlH_5 and $B_2AlH_6^+$ are similar to the most stable structure of $B_3H_6^+$. It indicates that the possibilities of hydrogen bridged structures are prominent in the mixed boron and aluminum three-membered-ring hydrides.

It is noteworthy that the most stable monoprotonated structure of $BAl_2H_3^{2-}$ is similar (in terms of position of the bridging hydrogens) to the most stable structures of B_2AlH_5, $B_2AlH_6^+$ and $B_3H_6^+$. It has lone pair on each Al atom, similar to the most stable structure of $BAl_2H_3^{2-}$. The di- and triprotonated structures of $BAl_2H_3^{2-}$ do not have lone pairs on aluminum atoms. The mono- and diprotonated structures of $Al_3H_3^{2-}$ are similar to the most stable structures of $B_3H_4^-$ and B_3H_5, respectively, but the bridging and the terminal hydrogens are not in the plane of the three-membered ring. The most stable structure of $Al_3H_6^+$ has a rather unusual structure. It has a planar tetracoordinated aluminum atom having a lone pair and two hexacoordinated aluminum atoms.

The most stable structures of $B_3H_6^+$, B_2AlH_5 and $BAl_2H_4^-$ and the trihydrogen-bridged structure of $Al_3H_3^{2-}$ show an interesting structural relationship (Figure 13). Substitution of one of the BH groups in $B_3H_6^+$ by Al^- having lone pair leads to the most stable structure of BAl_2H_5. Further substitution of the second BH group by Al^- results in the most stable structure of $BAl_2H_4^-$. Substitution of all the three BH groups by Al^- leads to a trihydrogen-bridged structure of $Al_3H_3^{2-}$ which is 7.9 kcal/mol higher in energy than the most stable structure at B3LYP/6-311+G* level of theory.[9] This structural relationship points out that there exist an isolobal analogy between trivalent boron and divalent aluminum anion (Figure 13).

Planarity versus Nonplanarity. The C_{3v} structure of $B_3H_6^+$ has been regarded as the first three-membered nonplanar 2π aromatic system.[10j] Sequential protonation of $B_3H_3^{2-}$ give rise to $B_3H_4^-$, B_3H_5 and $B_3H_6^+$, respectively (Figure 14).

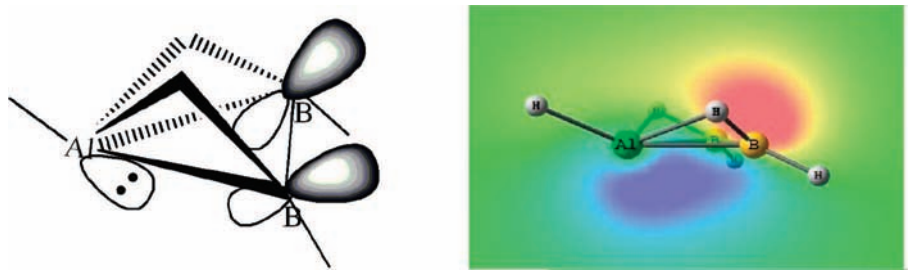

Figure 19. Representation of the out-of-plane 3c−2e (Al−B−B) bond in structure **3b.**

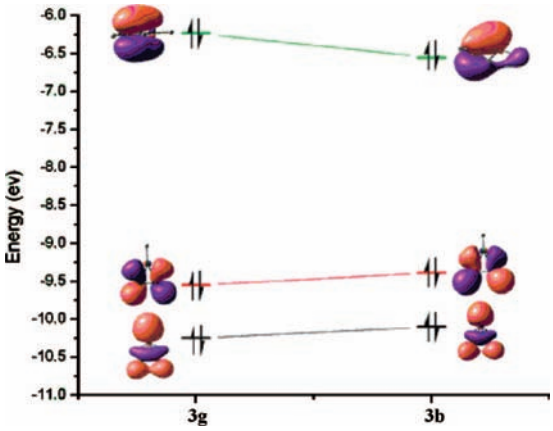

Figure 20. Correlation diagram between **3g** and **3b** showing the dramatic stabilization of the π-MO.

The most stable isomer of $B_3H_4^-$ has planar structure with one bridging hydrogen atom. Second protonation on $B_3H_3^{2-}$ generates B_3H_5, which has a planar 2π aromatic structure with two bridging hydrogen atoms. It is expected that the introduction of the third proton will give rise to a structure where all the three bridging and three terminal hydrogen atoms remain in the plane of the B_3 ring. But surprisingly it is found that the planar D_{3h} structure (Figure 15, **ii**) is a transition state and it is the nonplanar C_{3v} aromatic structure (Figure 15, **i**) that is the most stable isomer.[10j,9]

Why does the introduction of a third proton on $B_3H_3^{2-}$ produce a nonplanar structure as the most stable structure? The detailed electronic structure of B_3H_5 and $B_3H_6^+$ provides an explanation. The MOs of B_3H_5 can be constructed from B_3H_3 and H_2 fragment MOs. The three in-plane Walsh orbitals (a_1' and e') and the π-MO (a_2'') of the B_3H_3 ring are shown in Figure 16.

The interactions of degenerate e' orbitals of the B_3H_3 ring with the bonding and the antibonding MO of H_2 lead to the stabilization of the respective MOs. Similarly, the MOs of planar $B_3H_6^+$ can be constructed from B_3H_3 and H_3^+ fragment MOs.[10i] The degenerate MOs of the H_3^+ find a profitable interaction with the degenerate e' orbitals of B_3H_3. On the other hand, the a_1' orbitals of planar B_3H_3 and H_3^+ fragments do not interact strongly because they are nondirectional in nature. The a_1' orbital of H_3^+ cannot interact with the π-MO of the borocyclic ring also because it lies in the nodal plane of the π-MO. A correlation diagram between the planar and the nonplanar $B_3H_6^+$ shows a dramatic stabilization of the π-MO in going from planar (D_{3h}) to nonplanar (C_{3v}) structure.[10i] In the case of nonplanar structure the totally symmetric MO (a_1') of H_3^+ will find the right symmetry to interact with the π-MO of B_3H_3 ring and hence, stabilizes it.

Another contributor to the instability of the planar structure over the nonplanar structure is the steric repulsion that arises due to the introduction of the third bridging hydrogen atom. The distance between the terminal hydrogen (H_t) and the bridging hydrogen (H_b) in planar $B_3H_6^+$ is 1.88 Å, which is an unusually short H−H nonbonded distance.[27] This H_t-H_b nonbonded distance increases to 2.08 Å in the nonplanar structure and hence steric repulsion is minimized. Several examples (Figure 17, **iii**, **v**, **3a** and **4a**) are found where the nonplanar trihydrogen-bridged structures are more stable than the planar structures (Figure 17, **iv**, **vi**, **3m** and **4n**). In all the cases both the factors, such as the stabilization of the π-MO through the interaction with the out-of-plane bridging hydrogen atoms and the minimization of the steric repulsion between H_t and H_b contribute toward the stabilization of the nonplanar structures, though to different extents.

The bonding description, which is given earlier to explain the planar structure of B_3H_5, is inadequate to explain the bonding of the structures in which boron atoms of B_3H_5 are systematically replaced by aluminum atoms. For example, unlike B_3H_5 the planar C_{2v} isomer of B_2AlH_5 (Figure 18, **3g**) is a transition state. Planar structures of BAl_2H_5 (Figure 18, **viii**) and Al_3H_5 (Figure 18, **x**) have one and two imaginary frequencies respectively. The optimization of the planar C_{2v} structure of B_2AlH_5 along the direction of the imaginary frequency vector gives rise to a nonplanar structure (Figure 18, **3b**). Similar nonplanar structures are found to be minima for BAl_2H_5 (Figure 18, **vii**) and Al_3H_5 (Figure 18, **ix**) also.

As pointed out earlier, one of the reasons for the stability of the nonplanar structure is the stabilization of the π-MO through the interaction with the nonplanar bridging hydrogen atoms. If that is the governing factor for doubly hydrogen bridged structures, B_3H_5 should have preferred a nonplanar structure. But we have found that the nonplanar structure is not a stationary point on the PES of B_3H_5. It is true that in all the nonplanar structures the π-MO is stabilized, but the stabilization is not always because of the interaction with the out-of-plane bridging hydrogen atoms. The reason for the nonplanarity of the bridging and terminal hydrogen atoms in going from B_3H_5 to B_2AlH_5 is the propensity of aluminum to retain the lone pair. The bonding of the nonplanar isomer of B_2AlH_5 (Figure 18, **3b**) can be explained through the interaction of planar B_2H_4 fragment with the Al−H fragment. The lone pair of the Al−H fragment interacts with the vacant π-MO of the B_2H_4 fragment to make a π-type 3c−2e bond (Figure 19). This MO has minimal contribution from the bridging hydrogen atoms.

The observed deformation from the structure **3g** to **3b** can also be understood from its MO description using a correlation diagram, which depicts the stabilization of the π-MO in **3b** through the interaction with the lone pair orbital of aluminum (Figure 20).

Conclusions

We have studied the structure and bonding of $B_2AlH_n^m$ (n = 3−6, m = −2 to +1) by DFT and compared with $BAl_2H_n^m$,

homocyclic boron and aluminum analogues. Various numbers of coordination modes are observed in these species. A dramatic structural alteration is noted when boron atoms in $B_3H_n^m$ is systematically substituted by aluminum atoms. The most salient features are as follows: (1) The most stable structure for $B_3H_3^{2-}$ has a classical D_{3h} geometry, whereas the most stable structure of $B_2AlH_3^{2-}$ has bridging hydrogen atom at the Al−B bond and a lone pair on the aluminum atom. On the other hand, the most stable structures of $BAl_2H_3^{2-}$ and $Al_3H_3^{2-}$ have a lone pair on two aluminum atoms. The most stable structures result from a balance of the preference for lower coordination on aluminum, higher coordination on boron and a large number of the bridging hydrogen atoms between B−Al bonds. (2) The $B_2AlH_4^-$ shows similarities in the geometrical and the bonding patterns with the B_2SiH_4. (3) Nonplanarity of the hydrogen atoms with respect to the three-membered ring is found to be very common for Al and mixed B, Al three-membered ring systems. (4) The stabilization of the π-MO through the interaction with the nonplanar bridging hydrogens, the tendency of the aluminum atom to retain the lone pair and the minimization of the steric repulsion between the terminal and the bridging hydrogen atoms dictate the stability of the nonplanar hydrogen bridged structures over the planar analogues. (5) The most stable structure of $BAl_2H_4^-$ shows similarity in terms of the bridging hydrogen atoms with the most stable structures of B_2AlH_5, $B_2AlH_6^+$ and $B_3H_6^+$. (6) The most stable structures of $B_3H_6^+$, B_2AlH_5 and $BAl_2H_4^-$ and the trihydrogen-bridged structure of $Al_3H_3^{2-}$ show an isolobal analogy between trivalent boron and divalent aluminum anion.

Acknowledgment. We thank the Supercomputer Education and Research Centre (SERC) and the Centre for Modelling Simulation and Design (CMSD) for computational facilities and DST and BRNS for funding this research.

Supporting Information Available: Total energies, the number of imaginary frequencies, Cartesian coordinates, the structures and bond lengths of all the isomers of $B_2AlH_3^{2-}$, $B_2AlH_4^-$, B_2AlH_5, $B_2AlH_6^+$ and molecules **i**−**x**. This material is available free of charge via the Internet at http://pubs.acs.org.

References and Notes

(1) Kurth, F. A.; Schnöckel, R. A. E. H.; Downs, A. J.; Pulham, C. R. *J. Chem. Soc.* **1993**, *16*, 1302.

(2) Andrews, L.; Wang, X. *Science* **2003**, *299*, 2049.

(3) Breisacher, P.; Siegal, B. *J. Am. Chem. Soc.* **1964**, *86*, 5053.

(4) Wilkinson, F. A. C. a. G. *Advanced Inorganic Chemistry*, 2nd ed.; Wiley Interscience: New York, 1966.

(5) Lipscomb, W. N. *Boron Hydrides*; W. A. Benjamin: New York, 1963.

(6) Stock, A. E. *Hydrides of Boron and Silicon*; Cornell University: Ithaca, NY, 1933.

(7) (a) Adams, R. M. In *Boron, Metallo-Boron Compounds and Boranes*; Adams, R. M., Ed.; Wiley Interscience: New York, 1964; p 507. (b) Mutteries, E. L. *Boron Hydride Chemistry*; Academic Press: New York, 1975.

(8) (a) Friedman, L. B.; Dobrott, R. D.; Lipscomb, W. N. *J. Am. Chem. Soc.* **1963**, *85*, 3505. (b) Miller, N. E.; Forstner, J. A.; Muetterties, E. L. *Inorg. Chem.* **1964**, *3*, 690.

(9) Srinivas, G. N.; Anoop, A.; Jemmis, E. D.; Hamilton, T. P.; Lammertsma, K.; Leszczynski, J.; Schaefer, H. F. *J. Am. Chem. Soc.* **2003**, *125*, 16397.

(10) (a) Korkin, A. A.; Schleyer, P. v. R.; McKee, M. L. *Inorg. Chem.* **1995**, *34*, 961. (b) Schleyer, P. v. R.; Subramanian, G.; Dransfeld, A. *J. Am. Chem. Soc.* **1996**, *118*, 9988. (c) McKee, M. L.; Buhl, M.; Charkin, O. P.; Schleyer, P. v. R. *Inorg. Chem.* **1993**, *32*, 4549. (d) Krempp, M.; Damrauer, R.; DePuy, C. H.; Keheyan, Y. *J. Am. Chem. Soc.* **1994**, *116*, 3629. (e) Glukhovtsev, M. N.; Schleyer, P. v. R.; Hommes, N. J. R. V. E.; Carn-Eiro, J. W. D. M.; Koch, W. *Comput. Chem* **1993**, *14*, 285. (f) McKee, M. L. *Inorg. Chem.* **1999**, *38*, 321. (g) McKee, M. L. *J. Am. Chem. Soc.* **1995**, *117*, 8001. (h) Skancke, A.; Liebman, J. F. *J. Mol. Struct. (THEOCHEM)* **1993**, *280*, 75. (i) Jemmis, E. D.; Subramanian, G. *Inorg. Chem.* **1995**, *34*, 6559. (j) Jemmis, E. D.; Subramanian, G.; Srinivas, G. N. *J. Am. Chem. Soc.* **1992**, *114*, 7939.

(11) (a) Xie, Y.; Schreiner, P. R.; Schaefer, H. F.; Li, X.-W.; Robinson, G. H. *J. Am. Chem. Soc.* **1996**, *118*, 10635. (b) Li, X.-W.; Xie, Y.; Schreiner, P. R.; Gripper, K. D.; Crittendon, R. C.; Campana, C. F.; Schaefer, H. F.; Robinson, G. H. *Organometallics* **1996**, *15*, 3798. (c) Li, X.-W.; Pennington, W. T.; Robinson, G. H. *J. Am. Chem. Soc.* **1995**, *117*, 7578.

(12) Roseky, H. W. *Inorg. Chem.* **2004**, *43*, 7284.

(13) (a) Uhl, W. *Struct. Bonding (Berlin)*; Springer Verlag: Berlin, 2002; *Vol. 105*, pp 41−66. (b) Uhl, W.; Breher, F. *Eur. J. Inorg. Chem.* **2000**, 1. (c) Uhl, W.; Spies, T.; Koch, R.; Saak, W. *Organometallics* **1999**, *18*, 4598. (d) Cui, C.; Kopke, S.; Herbst-Irmer, R.; Roesky, H. W.; Noltemeyer, M.; Schmidt, H.-G.; Wrackmeyer, B. *J. Am. Chem. Soc.* **2001**, *123*, 9091.

(14) Cui, C.; Roesky, H. W.; Schmidt, H.-G.; Noltemeyer, M.; Hao, H.; Cimpoesu, F. *Angew. Chem., Int. Ed.* **2000**, *39*, 4274.

(15) Jemmis, E. D.; Parameswaran, P. *Chem. Eur. J.* **2007**, *13*, 2622.

(16) Hehre, W.; Radom, L.; Schleyer, P. v. R.; Pople, J. A. *Ab Initio Molecular Orbital Theory*; Wiley: New York, 1986.

(17) (a) Becke, A. D. *J. Chem. Phys.* **1993**, *98*, 5648. (b) Becke, A. D. *Phys. Rev. A* **1988**, *38*, 3098. (c) Lee, C.; Yang, W.; Parr, R. G. *Phys. Rev. B* **1988**, *37*, 785. (d) Vosko, S. H.; Wilk, L.; Nusair, M. *Can J. Phys* **1980**, *58*, 1200.

(18) Frisch, M. J.; Trucks, G. W.; Schlegel, H. B.; Scuseria, G. E.; Robb, M. A.; Cheeseman, J. R.; Montgomery,J. A., Jr.; Vreven, T.; Kudin, K. N.; Burant, J. C.; Millam, J. M.; Iyengar, S. S.; Tomasi, J.; Barone, V.; Mennucci, B.; Cossi, M.; Scalmani, G.; Rega, N.; Petersson, G. A.; Nakatsuji, H.; Hada, M.; Ehara, M.; Toyota, K.; Fukuda, R.; Hasegawa, J.; Ishida, M.; Nakajima, T.; Honda, Y.; Kitao, O.; Nakai, H.; Klene, M.; Li, X.; Knox, J. E.; Hratchian, H. P.; Cross, J. B.; Bakken, V.; Adamo, C.; Jaramillo, J.; Gomperts, R.; Stratmann, R. E.; Yazyev, O.; Austin, A. J.; Cammi, R.; Pomelli, C.; Ochterski, J. W.; Ayala, P. Y.; Morokuma, K.; Voth, G. A.; Salvador, P.; Dannenberg, J. J.; Zakrzewski, V. G.; Dapprich, S.; Daniels, A. D.; Strain, M. C.; Farkas, O.; Malick, D. K.; Rabuck, A. D.; Raghavachari, K.; Foresman, J. B.; Ortiz, J. V.; Cui, Q.; Baboul, A. G.; Clifford, S.; Cioslowski, J.; Stefanov, B. B.; Liu, G.; Liashenko, A.; Piskorz, P.; Komaromi, I.; Martin, R. L.; Fox, D. J.; Keith, T.; Al-Laham, M. A.; Peng, C. Y.; Nanayakkara, A.; Challacombe, M.; Gill, P. M. W.; Johnson, B.; Chen, W.; Wong, M. W.; Gonzalez, C.; Pople, J. A. *Gaussian 03*, revision C.02; Gaussian, Inc.: Wallingford, CT, 2004.

(19) (a) Fujimoto, H.; Hoffmann, R. *J. Phys. Chem.* **1974**, *78*, 1167. (b) Hoffmann, R. *Angew. Chem., Int. Ed. Engl.* **1982**, *21*, 711. (c) Reed, A. E.; Curtiss, L. A.; Weinhold, F. *Chem. Rev.* **1988**, *88*, 899.

(20) (a) Coester, F. *Nucl. Phys.* **1958**, *1*, 421. (b) Coester, F.; Kümmel, H. *Nucl. Phys.* **1960**, *17*, 477. (c) Bartlett, R. J. *J. Phys. Chem.* **1989**, *93*, 1697.

(21) (a) Lischka, H.; Koehler, H. J. *J. Am. Chem. Soc.* **1983**, *105*, 6646. (b) Colegrove, B. T.; Schaefer, H. F. *J. Phys. Chem.* **1990**, *94*, 5593.

(22) Subramanian, G.; Jemmis, E. D. *Chem. Phys. Lett.* **1992**, *200*, 567.

(23) Palagyi, Z.; Grev, R. S.; Schaefer, H. F., III. *J. Am. Chem. Soc.* **1993**, *115*, 1936.

(24) Jemmis, E. D. *J. Am. Chem. Soc.* **1982**, *104*, 7017.

(25) (a) Yu, T.; Cheng, T. M. H.; Kempter, V.; Lampe, F. W. *J. Phys. Chem.* **1972**, *76*, 3321. (b) Boo, B. H.; Armentrout, P. B. *J. Am. Chem. Soc.* **1987**, *109*, 3549.

(26) (a) Jemmis, E. D.; Prasad, B. V.; Tsuzuki, S.; Tanabe, K. *J. Phys. Chem.* **1990**, *94*, 5530. (b) Jemmis, E. D.; Prasad, B. V.; Prasad, P. V. A.; Tsuzuki, S.; Tanabe, K. *Proc. Ind. Acad. Sci. (Chem. Sci.)* **1990**, *102*, 107.

(27) Arunan, E.; Mandal, P. K. *J. Chem. Phys.* **2001**, *114*, 3880.

JP803894T